

Optical and electronic properties of an amorphous silicon-germanium alloy with a 1.28 eV optical gap

J. Kolodzey,^{a)} R. Schwarz,^{b)} S. Aljishi, V. Chu, D.-S. Shen, P. M. Fauchet, and S. Wagner

Department of Electrical Engineering, Princeton University, Princeton, New Jersey 08544

(Received 24 April 1987; accepted for publication 30 November 1987)

We report the deposition and comprehensive evaluation of a hydrogenated, fluorinated amorphous silicon-germanium alloy with an optical gap of 1.28 eV. This low-gap alloy of the *a*-Si_{1-x}Ge_x:H system possesses a small midgap defect density ($6.5 \times 10^{16} \text{ cm}^{-3}$), and useful electron ($\sigma_{\text{ph}}/\sigma_d = 23$) and hole ($L_D = 0.13 \mu\text{m}$) transport properties. The alloy was grown by radio-frequency plasma-enhanced decomposition of SiF₄, GeF₄, and H₂ in a reactor built to ultrahigh-vacuum specifications.

Alloys of hydrogenated amorphous silicon-germanium (*a*-Si_{1-x}Ge_x:H) have an optical energy gap (E_{opt}) that varies from 1.75 eV for unalloyed *a*-Si:H to 1.0 eV for *a*-Ge:H. Because of their potential low cost, wide choice of compatible substrate materials, and adjustable optical gap, these alloys are candidates for many device applications, such as long-wavelength absorbers in multijunction solar cells, and as photoreceptors for electrophotography using light-emitting diode sources.

Several groups have reported that low Ge content alloys with high optical gaps, $E_{\text{opt}} > 1.4 \text{ eV}$, can be used as charge collecting layers in solar cells with encouraging conversion efficiencies.¹⁻³ Higher Ge content, lower gap alloys with $E_{\text{opt}} < 1.4 \text{ eV}$ have been reported with poor transport properties, such as photo-to-dark conductivity ratios near 1, and with diffusion lengths and drift mobilities that are much smaller than in unalloyed *a*-Si:H.⁴⁻⁸ The variations in transport properties of alloys having identical Ge contents are commonly ascribed to variations in deposition technique. In this letter we describe the preparation of a fluorinated *a*-Si_{1-x}Ge_x:H,F alloy with $E_{\text{opt}} = 1.28 \text{ eV}$ and useful electronic properties.

The 1.28 eV gap *a*-Si_{1-x}Ge_x:H,F alloy film was prepared from fluorinated source gases and hydrogen in a stainless-steel, ultrahigh-vacuum deposition station as described elsewhere.⁹ The vacuum chamber degassing rate is $3 \times 10^{-7} \text{ Torr l s}^{-1}$, and a substrate load lock permits it to be kept evacuated continuously. Two stainless-steel electrodes are configured as a parallel plate diode. To avoid dust problems, a substrate is held upside down on the upper electrode, which is heated to typically 270 °C for deposition. Source gases are decomposed in a plasma excited by radio frequency at 13.56 MHz and with a substrate power density of 250 mW cm⁻². For the alloy reported here, the source gases (and their flow rates in standard cubic centimeters per minute) were SiF₄ (28 sccm), GeF₄ (0.55 sccm), and H₂ (4.5 sccm). Deposition pressure was 0.106 Torr, which needed to be precisely controlled to prevent film peeling. The film growth rate was 0.06 nm s⁻¹.

After loading the substrate, the station was pumped down for 15 h prior to deposition, while the temperature of the chamber external wall was maintained at 90 °C. The H₂O partial pressure was less than 10⁻⁹ Torr ($1.3 \times 10^{-7} \text{ Pa}$), measured with the use of a residual gas analyzer. A low background pressure of H₂O appears essential for a good-quality alloy.

The alloy substrate is a 1 in. \times 3 in. \times 1 mm slide of Corning 7059 glass. A 1 \times 1.5 in.² portion of the glass is precoated with 100 nm of evaporated Cr, which forms the back electrical contact for a Schottky barrier device fabricated by evaporating 10 nm of Pd through a mask over the deposited alloy. The Schottky device is used for time-of-flight and diffusion length measurements to be described later. The alloy on the bare glass substrate portion is used for optical and electrical conductivity measurements. Co-planar Cr ohmic contacts are evaporated on the alloy surface for conductivity measurements.

Our high Ge content alloys have tended to be microcrystalline with high dark conductivity, whereas the dark conductivity of our amorphous films is lower by several orders of magnitude.¹⁰ The 1.28 eV alloy was verified to be amorphous by the absence of x-ray diffraction peaks at the crystalline Si and Ge diffraction angles,¹¹ and by smooth bands in the Raman spectrum, indicating Ge-Ge, Ge-Si, and Si-Si bonds at wave numbers of 278, 390, and 480 cm⁻¹, respectively. To deposit Ge-rich alloys with an amorphous structure, we reduce the H₂ process gas flow rate to 4.5 sccm, down from 10 sccm used for low Ge content alloys.

Our optical and electrical measurement procedures are described elsewhere.⁹ The film thickness determined from infrared interference is $d = 1.2 \mu\text{m}$. The optical absorption coefficient α is determined from transmission and reflection for photon energies $h\nu$ above E_{opt} . For $h\nu$ below E_{opt} , α is determined by the constant photocurrent method.¹² The 1.28 eV value for E_{opt} is determined from the Tauc extrapolation of $\sqrt{\alpha h\nu}$ vs $h\nu$ and leads to an estimated Ge atomic fraction $x = 0.6$. Figure 1 shows Tauc plots of the 1.28 eV alloy and unalloyed *a*-Si:H,F at temperatures of 7 and 92 °C. For the alloy the optical gap drops with increasing T at a rate of -0.47 meV/K .

For $h\nu$ near E_{opt} , $\alpha = \alpha_0 \exp(E/E_0)$ has a characteristic Urbach energy E_0 determined by the valence band tail width.¹³ For the alloy we find $E_0 = 59 \text{ meV}$. The integrated

^{a)} Eastman Kodak Graduate Fellow. Present address: Department of Electrical and Computer Engineering, University of Illinois at Urbana-Champaign.

^{b)} Present address: Physik Department, Technische Universität München, Munich, West Germany.

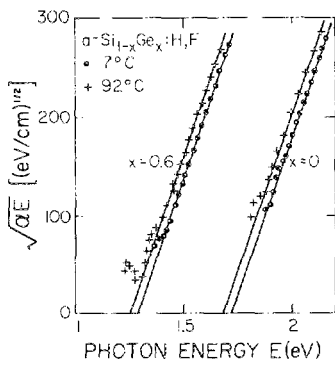


FIG. 1. Square root of optical absorption-photon energy product in the Tauc form vs photon energy E at temperatures of 7 and 92°C for the $a\text{-Si}_{1-x}\text{Ge}_x\text{:H,F}$ alloy and unalloyed $a\text{-Si:H,F}$ ($x = 0$). Extrapolation to the E axis yields the optical gap.

area under the low-energy shoulder of α vs $h\nu$ is proportional to the density of defect states (DOS) at midgap energies.¹⁴ With the use of a conversion factor for $a\text{-Si:H}$ ($1.9 \times 10^{16} \text{ cm}^{-2} \text{ eV}^{-1}$),¹⁵ the alloy DOS is $6.5 \times 10^{16} \text{ cm}^{-3}$.

Dark conductivity σ_d is measured in a vacuum oven, where the sample is first heated to 90°C . This procedure drives off surface water and yields reproducible values of σ_d . At 295 K , $\sigma_d = 1.9 \times 10^{-7} \text{ S cm}^{-1}$ and increases with temperature with an activation energy $E_{\text{cond}} = 0.59 \text{ eV}$. At room temperature, E_{cond} is about one-half E_{opt} , suggesting that the Fermi level E_F lies close to midgap. With the use of a vacuum cryostat, σ_d was measured from room temperature down to 125 K .¹⁶ Below 250 K , E_{cond} reduces to approximately 0.15 eV , and σ_d follows an expression, $\exp[-\text{const} \times T^{-1/4}]$, indicating conduction by variable range hopping.¹⁷

Photoconductivity σ_{ph} is measured by using monochromatic light with a wavelength of 750 nm and with the intensity adjusted to give a photon-absorption rate of $2 \times 10^{21} \text{ cm}^{-3} \text{ s}^{-1}$. At 295 K , $\sigma_{\text{ph}} = 4.3 \times 10^{-6} \text{ S cm}^{-1}$, resulting in a photo-to-dark conductivity ratio of 23. At 295 K , σ_{ph} increases with temperature with an activation energy $E_{\text{ph}} = 0.17 \text{ eV}$. Below 250 K , E_{ph} drops to 0.09 eV .

The drift mobility of electrons and mobility-lifetime products for electrons and holes are measured by using the time-of-flight (TOF) technique.¹⁸⁻²⁰ At 295 K , the electron drift mobility is $\mu_e = 1.9 \times 10^{-2} \text{ cm}^2 \text{ V}^{-1} \text{ s}^{-1}$ for the alloy. With the TOF technique, the mobility-lifetime products for electrons and holes $(\mu\tau)_{e,h}$ are determined from charge collection versus applied field.¹⁹ The $(\mu\tau)_{e,h}$ values are plotted versus temperature in Fig. 2. At room temperature, $(\mu\tau)_e$ for electrons is about an order of magnitude higher than $(\mu\tau)_h$ for holes. Dividing $(\mu\tau)_e$ by the independently determined value for μ_e gives the deep trapping lifetime $\tau_{d,e}$. We obtain $\tau_{d,e} = 6.8 \times 10^{-8} \text{ s}$ at 295 K . The drop in the activation energy of $(\mu\tau)_e$ below 250 K is consistent with the drop in the activation energies of dark and photoconductivities at this temperature, and indicates a change to hopping conduction. For holes the activation energy of $(\mu\tau)_h$ is constant

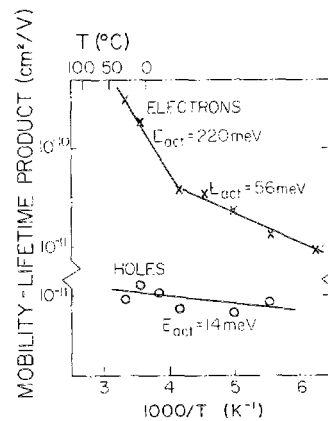


FIG. 2. Mobility-lifetime products for electrons and holes plotted vs inverse temperature for the 1.28 eV alloy.

over the temperature range of 155 to 300 K .

A second method to determine a mobility-lifetime product uses the bias dependence of the collection efficiency under steady-state uniformly absorbed light in a Schottky barrier structure.²¹ Our measurements for this quantity at room temperature yield $(\mu\tau)_{\text{coll}} = 4.5 \times 10^{-10} \text{ cm}^2 \text{ V}^{-1}$, which is approximately equal to the TOF-derived $(\mu\tau)_e$ for electrons.

A third method to determine a $\mu\tau$ value uses photoconductivity that is dominated by the transport of majority electrons. From the measured σ_{ph} and corresponding absorption rate, we get $(\eta\mu\tau_{\text{rec}})_{\text{photo}} = 1.34 \times 10^{-8} \text{ cm}^2 \text{ V}^{-1}$, which is larger than the values obtained by either TOF or charge collection. Here η is the quantum efficiency, and τ_{rec} is the recombination time. τ_{rec} is determined by the density of dangling bonds near midgap, and this is less than the density of deep traps, which determines the deep trapping lifetime relevant in a TOF measurement, $\tau_{d,e}$. A large density of states produces a small lifetime,²² and we expect that $\tau_{d,e} \ll \tau_{\text{rec}}$, which is consistent with the measurement $(\mu\tau)_e \ll (\eta\mu\tau_{\text{rec}})_{\text{photo}}$.

The ambipolar diffusion length L_D characterizes minority hole transport and is plotted in Fig. 3 for the 1.28 eV alloy and for 1.72 eV $a\text{-Si:H,F}$. L_D was measured over a range of temperatures by using the differential surface photovoltage technique.²³ The activation energy of the alloy is much less than for the $a\text{-Si:H,F}$, indicating that the peak in occupied hole traps is closer to the valence band edge for the alloy. It is interesting to compare the activation energies $(E_{\text{act}})_{\text{diff}}$ of diffusion length with that of $(\mu\tau)_h$ for holes from TOF, $(E_{\text{act}})_{h,\text{TOF}}$. We use the relation

$$L_D \sim [(kT/q)(\mu\tau)_h]^{1/2},$$

where kT is the thermal energy and q is the electronic charge. From this relation we may expect that $(E_{\text{act}})_{\text{diff}} = (1/2)(E_{\text{act}})_{h,\text{TOF}}$. Comparing room-temperature values for the alloy, we find instead that $(E_{\text{act}})_{\text{diff}} = 24 \text{ meV}$ is greater than $(E_{\text{act}})_{h,\text{TOF}} = 14 \text{ meV}$. The reason for the discrepancy is that L_D is measured under intense illumination, whereas $(\mu\tau)_h$ is measured under darkness, and so the appropriate $\mu\tau$ for the L_D equation is not $(\mu\tau)_h$ from TOF.

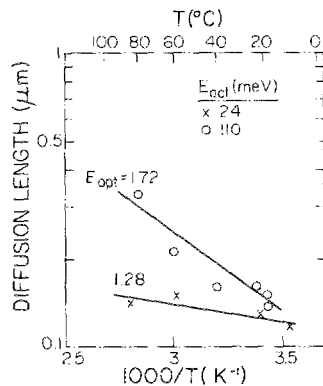


FIG. 3. Diffusion length plotted vs inverse temperature for the 1.28 eV alloy and unalloyed a -Si:H,F with 1.72 eV optical gap.

In summary, we have grown a low-gap a -Si,Ge:H,F alloy with a low-midgap defect density and high values for the photo-to-dark conductivity ratio and diffusion length. We attribute our result to careful adjustment of deposition parameters. The H_2O partial pressure was reduced by a long bakeout and pumpdown time prior to deposition. The deposition flow rate of H_2 was kept low to produce a truly amorphous structure. Electronic transport parameters were measured over a range of temperatures, and their activation energies were reported. The properties of this alloy are encouraging for the use of low-gap a -Si,Ge:H alloys in photovoltaic and other applications.

Special thanks to I. H. Campbell, Joao Conde, Cathy Lane, Sean Quinian, Ben Shapo, Dave Slobodin, and Z E. Smith who provided valuable assistance, and to Chris Wronski for encouragement and stimulating discussions. This work was supported by the Electric Power Research Institute under contract No. RP 2824-2.

¹G. Nakamura, K. Sato, and Y. Yukimoto, *Jpn. J. Appl. Phys.* **21**, Suppl. 21-2, 297 (1982); G. Nakamura, K. Sato, and Y. Yukimoto, in *16th IEEE Photovoltaic Specialists Conference Record* (IEEE, New York, 1982), p. 1331.

²J. Yang, R. Ross, R. Mohr, and J. P. Fournier, in *18th IEEE Photovoltaic Specialists Conference Record* (IEEE, New York, 1985), p. 1519.

³K. W. Mitchell, Y. H. Shing, and P. Yan, in *18th IEEE Photovoltaic Specialists Conference Record* (IEEE, New York, 1985), p. 894.

⁴K. Nozawa, Y. Yamaguchi, J. Hanna, and I. Shimizu, *J. Non-Cryst. Solids* **59&60**, 533 (1983).

⁵R. A. Rudder, J. W. Cook, Jr., and G. Lucovsky, *Appl. Phys. Lett.* **45**, 887 (1984).

⁶K. D. Mackenzie, J. R. Eggert, D. J. Leopold, Y. M. Li, S. Lin, and W. Paul, *Phys. Rev. B* **31**, 2198 (1985).

⁷J. Kolodzey, D. Slobodin, S. Aljishi, S. Quinlan, R. Schwarz, D.-S. Shen, P. M. Fauchet, and S. Wagner, *J. Non-Cryst. Solids* **77&78**, 897 (1985).

⁸F. Karg, W. Kruhler, M. Moeller, and K. v. Klitzing, *J. Appl. Phys.* **60**, 2016 (1986).

⁹J. Kolodzey, S. Aljishi, R. Schwarz, D. Slobodin, and S. Wagner, *J. Vac. Sci. Technol. A* **4**, 2499 (1986).

¹⁰D. Slobodin, J. Kolodzey, S. Aljishi, Y. Okada, V. Chu, D.-S. Shen, R. Schwarz, and S. Wagner, in *18th IEEE Photovoltaic Specialists Conference Record* (IEEE, New York, 1985), p. 1505.

¹¹D.-S. Shen, J. Kolodzey, D. Slobodin, J. P. Conde, C. Lane, I. H. Campbell, P. M. Fauchet, and S. Wagner, in *Proceedings of Materials Research Society*, edited by D. Adler, Y. Hamakawa, and A. Madan (MRS, Pittsburgh, 1986), Vol. 70, p. 301.

¹²M. Vanecek, J. Kocka, J. Stuchlik, Z. Kozisek, O. Stika, and A. Triska, *Sol. Energy Mater.* **8**, 411 (1983).

¹³T. Tiedje, J. M. Cebulka, D. L. Morel, and B. Abeles, *Phys. Rev. Lett.* **46**, 1425 (1981).

¹⁴W. B. Jackson and N. M. Amer, *Phys. Rev. B* **25**, 5559 (1982).

¹⁵Z. E. Smith, V. Chu, K. Shepard, S. Aljishi, D. Slobodin, J. Kolodzey, S. Wagner, and T. L. Chu, *Appl. Phys. Lett.* **50**, 1521 (1987).

¹⁶S. Aljishi and S. Wagner (unpublished).

¹⁷N. F. Mott and E. A. Davis, *Electronic Processes in Non Crystalline Materials*, 2nd ed. (Clarendon, Oxford, 1979), p. 345.

¹⁸T. Tiedje, C. R. Wronski, B. Abeles, and J. M. Cebulka, *Sol. Cells* **2**, 301 (1980).

¹⁹R. A. Street, *Phys. Rev. B* **27**, 4924 (1983).

²⁰S. Aljishi, Z. E. Smith, D. Slobodin, J. Kolodzey, V. Chu, R. Schwarz, and S. Wagner, *Proceedings of Materials Research Society*, edited by D. Adler, Y. Hamakawa, and A. Madan (MRS, Pittsburgh, 1986), Vol. 70, p. 269.

²¹C. R. Wronski, Z. E. Smith, S. Aljishi, V. Chu, K. Shepard, D.-S. Shen, R. Schwarz, D. Slobodin, and S. Wagner, *International Conference of Stability of Amorphous Silicon Alloy Materials and Devices*, Palo Alto, 1987 (AIP Conference Proceedings No. 157, New York, 1987), p. 70.

²²A. Rose, *Concepts in Photoconductivity and Allied Problems* (R. E. Krieger, Huntington, 1978).

²³R. Schwarz, D. Slobodin, and S. Wagner, *Appl. Phys. Lett.* **47**, 740 (1985).